

Physical-Layer Abstraction for Hybrid GNSS and 5G Positioning Evaluations

José A. del Peral-Rosado*, Olivier Renaudin*, Christian Gentner[†], Ronald Raulefs[†],
Enrique Domínguez-Tijero[‡], Alejandro Fernández-Cabezas[‡], Fernando Blázquez-Luengo[‡],
Gema Cueto-Felgueroso[‡], Alexander Chassaigne[§], David Bartlett[¶], Florin Grec^{||}, Lionel Ries^{||},
Roberto Prieto-Cerdeira^{||}, José A. López-Salcedo* and Gonzalo Seco-Granados*

*IEEC-CERES, Universitat Autònoma de Barcelona (UAB), Bellaterra, Spain

Email: {JoseAntonio.delPeral, Olivier.Renaudin, Jose.Salcedo, Gonzalo.Seco}@uab.cat

[†]German Aerospace Center (DLR), Wessling, Germany

Email: {Christian.Gentner, Ronald.Raulefs}@dlr.de

[‡]GMV, Tres Cantos, Spain

Email: {edominguez, alfernandez, fbblazquez, gcueto}@gmv.com

[§]Telefónica I+D, Madrid, Spain

Email: alexander.chassaigne@telefonica.com

[¶]u-blox AG, Cambourne, The UK

Email: david.bartlett@u-blox.com

^{||}European Space Agency (ESA), Noordwijk, The Netherlands

Email: {Florin-Catalin.Grec, Lionel.Ries, Roberto.Prieto.Cerdeira}@esa.int

Abstract—Hybridization of Global Navigation Satellite Systems (GNSS) and fifth generation (5G) cellular positioning is foreseen as a key solution to fulfill high-accuracy positioning requirements in future use cases, such as autonomous vehicles. The evaluation of the hybrid positioning capabilities implies the physical-layer simulation of observables from both GNSS and 5G technologies. In order to ease the complexity of the resulting system-level simulations, a physical-layer abstraction of GNSS and 5G ranging observables is here proposed. The abstraction of GNSS ranging observables is based on a Gaussian-distributed model of the errors sources, while the abstraction of 5G ranging observables is based on the interpolation of the cumulative density function (CDF) of the ranging errors for certain propagation conditions and signal-to-noise (SNR) levels. Thanks to the exploitation of the proposed physical-layer abstraction, low-complexity system-level simulations are performed to assess the positioning capabilities of GNSS and 5G downlink time-difference of arrival (DL-TDoA) in urban macro-cell (UMa) environments. The simulation results indicate the need to adopt hybrid solutions based on multiple GNSS constellations and 5G DL-TDoA with 100-MHz bandwidth, in order to ensure a horizontal positioning accuracy below 5 m for 95% of cases in outdoor urban environments.

Index Terms—Hybrid positioning, GNSS, 5G, physical-layer abstraction, system-level simulations.

I. INTRODUCTION

High-accuracy positioning is envisaged as one of the main performance requirements in fifth generation (5G) networks [1]. The baseline positioning requirement is mainly based on a horizontal positioning accuracy below 10 m for the 95% of cases over outdoor and indoor scenarios. This is a stringent requirement with respect to the existing regulatory requirements for emergency services [2], based on a horizontal accuracy below 50 m for the 80% of cases. Thus,

the combination of 5G with additional technologies, such as Global Navigation Satellite Systems (GNSS), is expected to be necessary to overcome this major challenge, especially in harsh urban environments.

Towards the fulfilment of high-accuracy requirements, the 5G standardization has initiated the support of stand-alone and hybrid positioning methods in [2]. This study concludes that 5G-based positioning methods are shown to only meet regulatory requirements, mainly due to the presence of network synchronization errors, while the hybridization of GNSS and 5G achieves the baseline 10-m accuracy requirement. Nonetheless, hybrid positioning methods need further study in order to target higher accuracy levels [1], such as sub-meter accuracy on the 99% of cases.

The evaluation of hybrid positioning methods implies the physical-layer simulation of multiple technologies, which typically increases the complexity of the simulations. In order to simplify these simulations, hybrid evaluation methodologies are proposed in [3] and [4], based on the physical-layer abstraction of GNSS code observables. These methodologies are further extended in this work with the abstraction of 5G observables for downlink time-difference of arrival (DL-TDoA). Then, the proposed physical-layer abstraction of both GNSS and 5G observables is here exploited to assess the achievable hybrid positioning performance.

II. STANDARD SIMULATION ENVIRONMENTS

The simulation environments under study are defined based on standard specifications. This section describes the use of these standard environments for the simulation of GNSS and 5G positioning over urban areas.

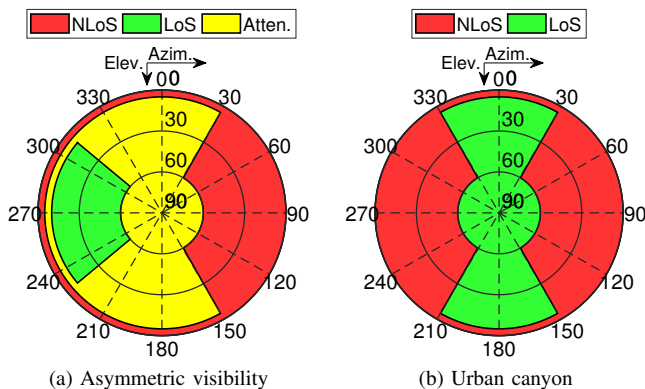


Fig. 1. Satellite visibility conditions based on ETSI TS 103.246-3 [5].

A. Satellite Environments

A typical representation of satellite propagation environments is based on a two-ray model under specific satellite visibility conditions, as it is adopted in ETSI TS 103.246-3 [5] for the definition of GNSS performance requirements. This ETSI specification defines three satellite operational environments based on sky attenuation conditions, i.e., open sky, asymmetric visibility (AV) and urban canyon (UC) conditions. That is, specific signal attenuation levels are defined for each possible elevation and azimuth between receiver and satellite. This approach simplifies the simulation environments by focusing on specific and representative scenario conditions determined by the GNSS visibility.

Our study considers the ETSI specification of AV and UC environments, in order to define the satellite propagation conditions over urban environments. As it is shown in Figure 1, the asymmetric case represents a satellite environment with higher satellite visibility than in the urban canyon case. Using this simplified approach, the elevation and azimuth of the satellite is sufficient to determine the line-of-sight (LoS) and non-LoS (NLoS) conditions, including an additional attenuation in certain LoS conditions.

B. Cellular Environments

The 3GPP standard defines four main cellular environments depending on the network deployment, i.e., rural macro-cell (RMa), urban macro-cell (UMa), urban micro-cell (UMi) street canyon, and indoor hotspot (InH) or indoor office. These environments are simulated based on the channel models defined in [6]. These simulations follow the concept of user equipment (UE) drops, in which UEs are randomly placed within the coverage area of the predefined deployment scenario. Then, the distance between base station (BS) and UE is used to determine the propagation conditions based on the distance-dependent LoS probability and pathloss models. Depending on these conditions, the multipath channel is stochastically generated following the tabulated channel parameters in [6]. Hence, each UE drop is an independent single statistical event. A sufficiently high number of drops has therefore to be drawn, usually through Monte-Carlo simulations, in order to obtain a statistical validity of the aggregated results expressed

in the form of appropriate metrics. This stochastic channel modeling is later exploited in Section III for the physical-layer abstraction of cellular observables, in order to ease the simulation complexity.

Nonetheless, the 3GPP channel models lack certain representativity or suitability for positioning due to the absence of NLoS bias. As it is discussed in [4], the path delays generated according to [6] are normalized to the first arrival path as

$$\tau = \text{sort}(\tau' - \min(\tau')), \quad (1)$$

where τ' are the stochastically-generated path delays. This normalization is only valid for LoS conditions. Thus, in order to study the impact of the NLoS bias, the path delay normalization is here removed as

$$\tau = \text{sort}(\tau'). \quad (2)$$

Since this modification is not validated experimentally, this simple approach is only intended to show the significance of the NLoS bias for positioning evaluations.

III. PHYSICAL-LAYER ABSTRACTION OF OBSERVABLES

The physical-layer abstraction of observables is here referred as the process to model observables obtained from physical-layer simulations or experimental measurements, in order to later generate observables without performing physical-layer simulations or measurements. This approach allows to considerably ease system-level simulations, based on the predefined observable models obtained from the physical-layer abstraction. This section describes the physical-layer abstraction proposed for GNSS and 5G observables.

A. GNSS Observables

The GNSS measurement errors can be classified between non-local errors, i.e., satellite orbits, satellite clocks and atmospheric effects, and local errors, i.e., loss of satellite tracking, multipath caused by signal reflections on nearby objects, NLoS tracking (or tracking of obstructed satellites by the receiver) and receiver noise. Since these errors sources can be considered to be independent random variables, they can be grouped in a single additive white Gaussian noise (AWGN) contribution with variance equal to the sum of the variances of each contribution. The resulting ranging error is called the User Equivalent Range Error (UERE), which is typically used to analyze the expected GNSS performance. Thus, the physical-layer abstraction of GNSS code observables is based on the UERE analysis, by assuming code-based pseudoranges obtained with dual-frequency GNSS receivers.

Let us model the k -th GNSS code pseudorange as

$$\hat{\rho}_{\text{GNSS},k} = c \cdot \hat{\tau}_{\text{GNSS},k} = \|\mathbf{x}_{\text{sat},k} - \mathbf{x}_{\text{UE}}\| + c \cdot \delta t_{\text{GNSS}} + e_{\text{sat},k}, \quad (3)$$

where $\hat{\tau}_{\text{GNSS},k}$ is the time-of-flight of the GNSS signal, $\mathbf{x}_{\text{sat},k} = [x_{\text{sat},k}, y_{\text{sat},k}, z_{\text{sat},k}]$ is the satellite position, $\mathbf{x}_{\text{UE}} = [x_{\text{UE}}, y_{\text{UE}}, z_{\text{UE}}]$ is the UE position, c is the speed of light, δt_{GNSS} is the clock offset of the UE (referenced to a GNSS time), and $e_{\text{sat},k}$ is the pseudorange error. The inter-system

TABLE I
1- σ ERROR BUDGETS FOR GNSS PHYSICAL-LAYER ABSTRACTION.

| Error source (1- σ , m) | Elevation (degrees) | | | | | | | | |
|-----------------------------------|---------------------|------|------|------|------|------|------|------|------|
| | 5 | 10 | 15 | 20 | 30 | 40 | 50 | 60 | 90 |
| GPS $\sigma_{\text{orb,clk}}$ | 0.95 | 0.95 | 0.95 | 0.95 | 0.95 | 0.95 | 0.95 | 0.95 | 0.95 |
| Galileo $\sigma_{\text{orb,clk}}$ | 0.67 | 0.67 | 0.67 | 0.67 | 0.67 | 0.67 | 0.67 | 0.67 | 0.67 |
| GLONASS $\sigma_{\text{orb,clk}}$ | 1.8 | 1.8 | 1.8 | 1.8 | 1.8 | 1.8 | 1.8 | 1.8 | 1.8 |
| Beidou $\sigma_{\text{orb,clk}}$ | 2 | 2 | 2 | 2 | 2 | 2 | 2 | 2 | 2 |
| σ_{iono} | 0.08 | 0.07 | 0.06 | 0.06 | 0.05 | 0.04 | 0.03 | 0.03 | 0.03 |
| σ_{trop} | 1.35 | 0.75 | 0.51 | 0.39 | 0.27 | 0.21 | 0.18 | 0.16 | 0.14 |
| GPS σ_w | 0.75 | 0.63 | 0.52 | 0.42 | 0.30 | 0.22 | 0.18 | 0.18 | 0.18 |
| Galileo σ_w | 0.75 | 0.63 | 0.52 | 0.42 | 0.30 | 0.22 | 0.18 | 0.18 | 0.18 |
| GLONASS σ_w | 1.05 | 0.88 | 0.72 | 0.58 | 0.42 | 0.30 | 0.25 | 0.25 | 0.25 |
| Beidou σ_w | 0.75 | 0.63 | 0.52 | 0.42 | 0.30 | 0.22 | 0.18 | 0.18 | 0.18 |
| σ_{mp} | 4.61 | 4.37 | 4.22 | 4.14 | 4.05 | 4.02 | 4.01 | 4.00 | 4.00 |

bias between GNSS constellations is assumed to be known and corrected, because this parameter is stable enough to be estimated using information from long intervals. The pseudo-range error is assumed Gaussian-distributed with zero-mean and UERE variance as $e_{\text{sat},k} \sim \mathcal{N}(0, \sigma_{\text{UERE},k}^2(\theta_k))$. The UERE variance is calculated as function of the k -th visible satellite elevation θ_k from a certain constellation, by using the standard deviation of each error source defined in Table I. As a result, the UERE variance from the k -th satellite is

$$\sigma_{\text{UERE},k}^2(\theta_k) = \sigma_{\text{orb,clk}}^2(\theta_k) + \sigma_{\text{iono}}^2(\theta_k) + \sigma_{\text{trop}}^2(\theta_k) + \sigma_w^2(\theta_k) + \sigma_{\text{mp}}^2(\theta_k), \quad (4)$$

where $\sigma_{\text{orb,clk}}^2(\theta_k)$ is the orbit and clock error variance, $\sigma_{\text{iono}}^2(\theta_k)$ is the residual ionosphere error variance, $\sigma_{\text{trop}}^2(\theta_k)$ is the residual troposphere error variance, $\sigma_w^2(\theta_k)$ is the AWGN receiver noise error variance, $\sigma_{\text{mp}}^2(\theta_k)$ is the multipath error variance. The non-local 1- σ error budgets, i.e., $\sigma_{\text{orb,clk}}$, σ_{iono} and σ_{trop} , employed in this physical-layer abstraction of GNSS observables are obtained or extrapolated from several sources [7]–[17], and by considering dual-frequency GNSS receivers. Regarding the local errors, i.e., σ_w and σ_{mp} , the receiver noise values are obtained from what can be provided by an average GNSS receiver [15]. The values employed for each error source are considered to be representative in average during long periods of time, different locations and for average GNSS receivers, which means that there could be situations or receiver types for which the errors would be above or below those figures. Nevertheless, the total GNSS error budget would not suffer major changes so it is considered representative.

The GNSS outliers due to NLoS bias are usually detected, and discarded or down-weighted by the GNSS navigation algorithms, thanks to the high amount of observables with multiple constellations. Thus, the physical-layer abstraction of GNSS code observables assumes that NLoS biases have been filtered out so the results are obtained with GNSS satellites in LoS conditions with a representative multipath error. For those LoS attenuated conditions, such as in Figure 1a, the attenuation is here simulated by doubling the standard deviation of the AWGN receiver noise error, i.e., $\sigma_{w,\text{atten}}^2(\theta_k) = (2 \cdot \sigma_w(\theta_k))^2$.

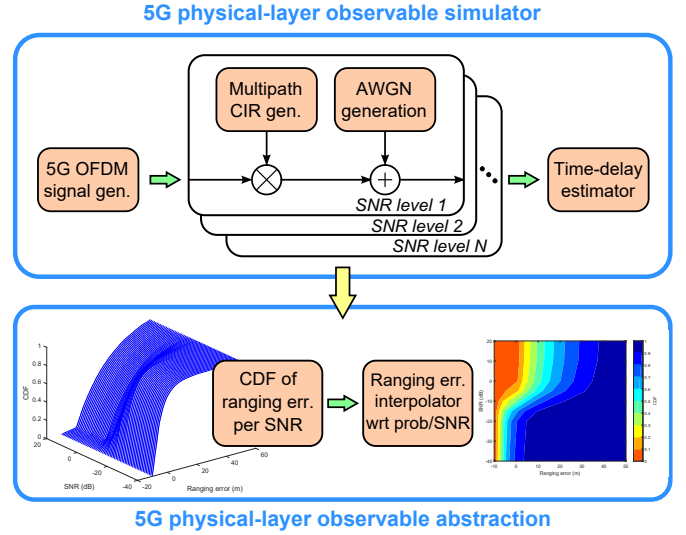


Fig. 2. Architecture of 5G physical-layer abstraction of ranging errors.

B. 5G Observables

The physical-layer abstraction of 5G ranging observables is described in the two-step procedure shown in Figure 2. First, the received physical 5G signal is simulated to estimate the ranging error for different signal-to-noise (SNR) levels. Then, the cumulative density function (CDF) of the resulting ranging errors per SNR level is computed and interpolated over the probability and SNR axis. The ranging error interpolator is finally used to generate 5G ranging observables given a certain SNR level and probability. Although this study considers a downlink 5G physical-layer simulator, the proposed approach can be applied to both uplink and downlink transmissions for simulated and experimental ranging measurements.

Let us model the k -th 5G ranging observable as

$$\hat{\rho}_{5G,k} = c \cdot \hat{\tau}_{5G,k} = \|\mathbf{x}_{\text{BS},k} - \mathbf{x}_{\text{UE}}\| + c \cdot \delta t_{5G} + e_{\text{sync},k} + e_{\text{TDE},k}, \quad (5)$$

where $\hat{\tau}_{5G,k}$ is the time-of-flight of the 5G signal, $\mathbf{x}_{\text{BS},k} = [x_{\text{BS},k}, y_{\text{BS},k}, z_{\text{BS},k}]$ is the k -th BS position, δt_{5G} is the clock offset of the 5G module (referenced to a GNSS time), $e_{\text{sync},k}$ is the network synchronization error, and $e_{\text{TDE},k}$ is the time-delay estimation (TDE) error. As in [2], the network synchronization error is here modeled as a truncated Gaussian distributed random variable with zero mean and standard deviation σ_{sync} within the interval of values $[-2 \cdot \sigma_{\text{sync}}, 2 \cdot \sigma_{\text{sync}}]$.

The downlink 5G physical-layer simulator is based on the dedicated transmission of orthogonal frequency division multiplexing (OFDM) pilot signals, i.e., positioning reference signal (PRS) with a frequency reuse factor of six, and the channel models in [6]. The received signal is simulated by convolving only one OFDM PRS symbol with a channel realisation, and by adding AWGN for a certain SNR level. Then, the threshold-based estimator in [3] is used to obtain the TDE error $e_{\text{TDE},k}$ as the time-delay measurement of the

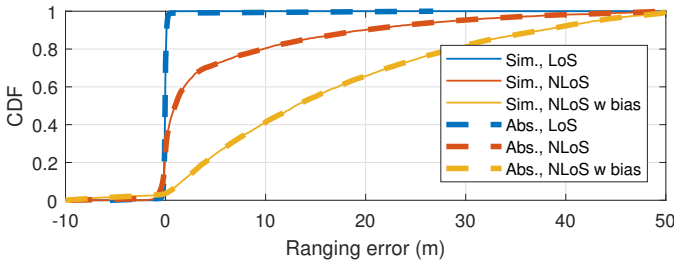


Fig. 3. CDF of ranging errors for UMa environment with SNR of 20 dB and 100-MHz PRS bandwidth at a carrier frequency of 4 GHz.

first correlation peak above a threshold, which is here defined 6 dB below the maximum peak over a correlation window.

The 5G physical-layer observable generation is performed through Monte-Carlo simulations, in order to obtain an accurate CDF of the ranging errors. Considering the independence of the technical report (TR) 38.901 channel parameters with the distance between UE and BS, the ranging errors can be modeled based on the LoS condition and SNR level. Thus, the abstraction procedure is repeated for LoS and NLoS conditions within the set of expected SNR values. In addition, as it is discussed in Section II-B, a modification to the TR 38.901 channel model is added in order to consider the NLoS bias. As example, the cellular UMa environment is considered with a 5G PRS system bandwidth of 100 MHz, resulting in the CDF of ranging errors shown in Figure 3. These results indicate the high ranging accuracy achievable in LoS conditions, while the NLoS bias has a significant impact on the ranging errors, which mainly limit the 5G positioning performance.

The physical-layer abstraction of the ranging observables is achieved thanks to the interpolation of the CDF of ranging errors. This interpolation is performed in the ranging error domain, by considering the known SNR levels and probabilities of the CDF. Since the probabilities of the ranging errors do not follow a regular grid, a two-dimensional (2D) scattered interpolation is performed with CDF of ranging errors obtained for the set of SNR levels. This interpolation results in a function or model that can be later evaluated for a certain SNR level and probability. Considering the UMa environment example with 100-MHz bandwidth, the 2D interpolation functions of the CDF ranging errors are shown in Figure 4 for LoS and NLoS conditions including the NLoS bias. As it can be noticed, the ranging errors are mainly dominated by multipath for SNR levels above -10 dB. In addition, the dominant LoS path for LoS channels shows a SNR gain around 5 dB with respect to the spread energy of NLoS channels.

These 2D interpolation functions are used as follows. First, the SNR level is computed for certain propagation conditions. Then, a random probability variable is drawn from a uniform distribution between 0 and 1. Using the 2D interpolation functions, these SNR and probability values yield a corresponding ranging error, whose value will be used for the system-level simulation. As it is shown in Figure 3, the CDF of the observables generated with the abstraction process perfectly matches those CDF obtained with physical-layer simulations.

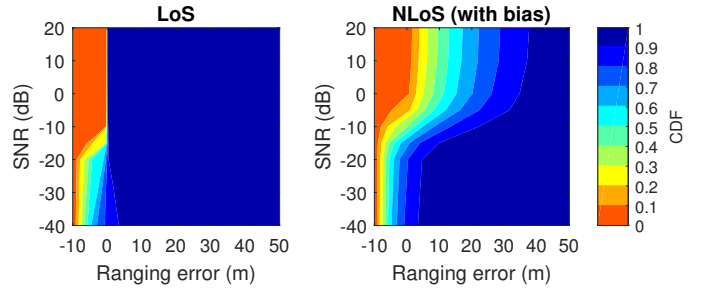


Fig. 4. 2D-interpolated CDF of ranging errors for LoS and NLoS conditions (including NLoS bias) over UMa environments.

The physical-layer abstraction of 5G observables helps to ease the simulation of ranging observables, by characterizing the ranging errors for specific propagation conditions, channel models, SNR levels and time-delay estimator. Although this abstraction process is here applied to ranging observables, the proposed approach can also be extrapolated to other observables. For instance, angle observables can also be abstracted with an additional dimension for the orientation between transmitter and receiver. The application of the proposed approach for other position-related observables is left for future work.

IV. SYSTEM-LEVEL SIMULATION RESULTS

This section presents system-level simulation results of hybrid GNSS and 5G DL-TDoA positioning, by taking advantage of the proposed physical-layer abstraction of observables. The low-complexity of these system-level simulations eases the evaluation of GNSS, 5G and hybrid positioning capabilities.

A. Evaluation Methodology

The evaluation methodology of the system-level simulations are based on the procedure proposed in [4]. The evaluations consider a UMa cellular deployment with inter-site distance (ISD) of 500 m and wrap-around of BSs [2]. The 5G system is assumed to operate a dedicated PRS transmission of 100 MHz with ideal PRS muting at a carrier frequency of 4 GHz. The four main GNSS constellations are simulated with full operational capabilities by using an orbiter generator, i.e., GPS with 24 satellites, Galileo with 27 satellites, GLONASS with 24 satellites and Beidou with 27 satellites. The UEs are dropped following a rectangular grid with 50-m resolution over a 500 m² evaluation area, resulting in 121 UE positions.

The GNSS observables are simulated using the physical-layer abstraction described in Section III-A. First, the ETSI AV or UC satellite environment is used to determine the LoS conditions of the simulated satellites. Second, the visible (or LoS) satellite positions are transformed to local coordinates. Then, the UERE variance is computed for each visible satellite. Finally, the GNSS code observable is generated by summing the distance between UE and satellite with a constant UE clock offset and a zero-mean Gaussian-distributed random variable with UERE variance. For each simulation, the street orientation of the ETSI satellite environment is shifted with a uniform random angle between 0 and 180 degrees.

The 5G DL-TDoA observables are simulated using a five-step procedure. First, the LoS conditions of the 5G ranging observables are obtained based on the distance-dependent LoS probability for UMa environments. Second, the SNR level of each observable is computed with a 3GPP-like link budget, as in [18], by using the UMa scenario parameters defined in [2]. Third, the ranging observables are limited to the six most powerful BSs. Fourth, the ranging observables are generated following the physical-layer abstraction proposed in Section III-B, by using as input the LoS conditions, the SNR levels and the probabilities obtained from uniformly-distributed random variables between 0 and 1. Finally, the n -th 5G DL-TDoA observable is computed as the time difference of ranges from the serving and neighbour BSs as $\rho_{\text{DL-TDoA},n} = \rho_{5\text{G},1} - \rho_{5\text{G},(n+1)}$ for $1 \leq n \leq 5$, where the first range corresponds to the most powerful BS.

The three-dimensional (3D) position estimation is based on a weighted least squares (WLS) algorithm with the available GNSS code and 5G DL-TDoA observables. A tightly-coupled WLS approach is adopted for hybrid solutions, which could be computed at the UE or at a network server. The weighting coefficients are described within the different evaluation cases. The CDF of the horizontal positioning accuracy is here used as the metric to assess the positioning performance.

The system-level evaluations are performed over 1000 Monte-Carlo simulations for each of the 121 UE dropped positions. For each simulation, the number of visible GNSS satellites can range from around 5 to 20 satellites depending on the number of constellations and environment, while the number of BSs is here fixed to six. As a result, the number of physical-layer simulations is very significant. Furthermore, channel simulations can be very time consuming due to a high number of multipath components. Thus, physical-layer simulations are expected to imply a high computation time within system-level simulations. By using the proposed physical-layer abstraction, the simulation time of the ranging observables becomes negligible with respect to the simulation of both GNSS and 5G physical layers. Thus, this approach eases the system-level evaluations of the hybrid GNSS and 5G positioning capabilities.

B. Multi-GNSS Positioning Capabilities

The impact of the GNSS visibility is first assessed by comparing the positioning performance of single and multiple constellations. Considering a single constellation, i.e., GPS, the number of visible satellites is around 5 and 3 satellites for AV and UC environments, respectively. The GNSS visibility significantly increases with multiple constellations, i.e., all four GNSS, resulting in more than 20 visible satellites and around 15 for AV and UC environments, respectively. The position accuracy is then computed for single- and multi-GNSS configurations, by considering the WLS approach with known UERE variance for each observable. As it is shown in Figure 5, the positioning availability of the single-GNSS approach is severely degraded in UC environments due to the lack of visible satellites, while the multi-GNSS approach

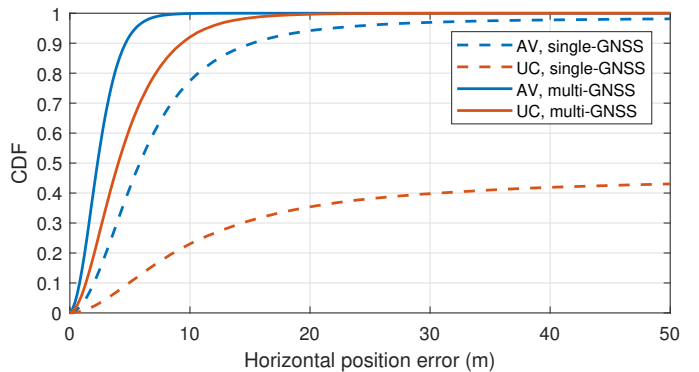


Fig. 5. Horizontal positioning accuracy for AV and UC satellite environments with single- and multi-GNSS solutions.

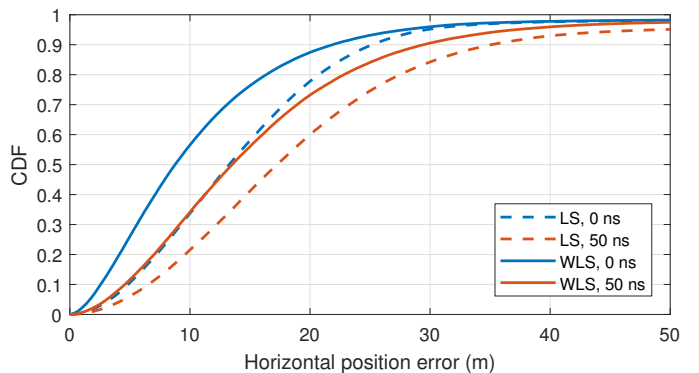


Fig. 6. Horizontal positioning accuracy for UMa cellular environment (including NLoS bias) using LS and WLS solutions with 100-MHz bandwidth.

reaches a 100% positioning availability. Nonetheless, multi-GNSS solutions can only ensure a position accuracy below 10 m for 95% of cases in AV environments. This is due to the limited accuracy of GNSS code observables in urban environments, which are here modeled with an UERE standard deviation above 4 m, and the reduced GNSS visibility in UC environments.

C. Stand-alone 5G DL-TDoA Positioning Algorithms

The impact of the propagation and network synchronization errors is assessed for stand-alone 5G DL-TDoA positioning. This assessment is performed for UMa environment including the NLoS bias with perfect synchronization and with a synchronization error of 50-ns standard deviation. The positioning algorithm is then evaluated with no prior information or with full information of the ranging errors. That is, a least-squares (LS) positioning algorithm, i.e., equal weights between observables, is compared with the WLS approach, i.e., using the absolute ranging errors within the weighting matrix. As it can be seen in Figure 6, there is a minor improvement on the use of WLS approach with respect to the LS approach. This is due to the predominance of NLoS conditions in the UMa environment, i.e., the LoS probability is as low as 35% for a distance of 100 m from UE to BS, and due to the significant synchronization error.

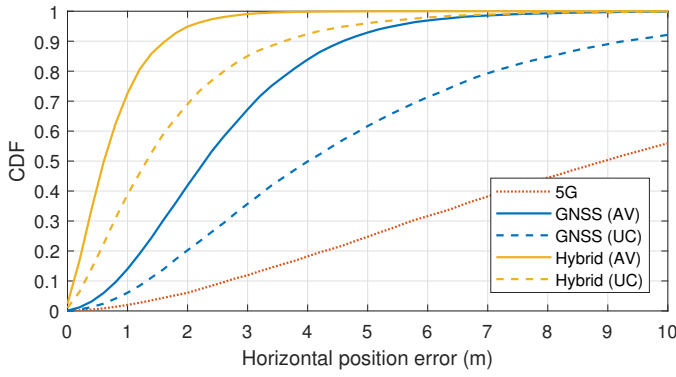


Fig. 7. Horizontal positioning accuracy for UMa cellular environment (including NLoS bias) with perfect network synchronization and AV and UC sky conditions using WLS solutions with known ranging errors.

D. Hybrid GNSS and 5G DL-TDoA Positioning Performance

The positioning limits of stand-alone GNSS and 5G can be overcome with their fusion in a tightly-coupled positioning algorithm, as in [3] and [4]. The five DL-TDoA observables over UMa environment (including NLoS bias) with 100-MHz PRS and perfect network synchronization are combined with multi-GNSS observables obtained over AV and UC sky conditions. Full information of the absolute ranging errors is considered for both GNSS and 5G observables within the weighting matrix of the WLS algorithm. As it is shown in Figure 7, there is a significant improvement of the hybrid approach with respect to the stand-alone positioning solutions in both AV and UC sky conditions, resulting in a horizontal accuracy below 5 m in the 95% of cases. This significant improvement is achieved thanks to the exploitation of high-accuracy 5G LoS observables in combination with the high number of multi-GNSS observables. Therefore, hybrid GNSS and 5G solutions are expected to have a key role on the achievement of sub-meter localization over urban areas. Nonetheless, further improvements may be necessary, such as with higher density of 5G BSs and high-accuracy carrier-phase GNSS measurements.

V. CONCLUSIONS

A physical-layer abstraction of ranging observables is proposed in this paper, in order to ease the evaluation of hybrid Global Navigation Satellite Systems (GNSS) and fifth generation (5G) positioning capabilities. The goal of this physical-layer abstraction is to reduce the complexity of system-level simulations, especially when physical-layer observables need to be obtained from two different technologies as GNSS and 5G. The abstraction of GNSS ranging observables is adopted from the literature based on the User Equivalent Range Error (UERE) analysis, which models the GNSS code observable error as a function of the satellite elevation. The physical-layer abstraction of 5G ranging observables is here proposed based on the interpolation of the cumulative density function (CDF) of time-delay errors, obtained under certain line-of-sight (LoS) conditions, signal-to-noise ratio (SNR) levels and propagation channel model with a threshold-based estimator. The pro-

posed physical-layer approach is exploited to perform Monte-Carlo simulations of the horizontal positioning performance of GNSS, 5G and hybrid solutions. The GNSS system-level simulation results show that multiple GNSS constellations are required to achieve a 100% positioning availability in urban canyons. Considering urban macro-cell (UMa) deployments, the predominance of non-LoS (NLoS) propagation conditions and network synchronization errors limit the positioning performance of 100-MHz 5G DL-TDoA solutions. Thus, hybrid GNSS and 5G is shown to achieve the best performance in all configurations by significantly improving the positioning performance of GNSS and 5G stand-alone solutions. The hybrid solution ensures a horizontal accuracy below 5 m on the 95% of cases. Still, further enhancements on both technologies, such as on 5G network density and high-accuracy GNSS observables, are needed to achieve sub-meter localization.

ACKNOWLEDGMENT

This work was supported in part by ESA EGEP programme under GINTO5G (GNSS Integration into 5G Wireless Networks) project and in part by the Spanish Ministry of Science, Innovation and Universities under project TEC2017-89925-R.

REFERENCES

- [1] 3GPP TS 22.261, "Service requirements for next generation new services and markets," Rel. 16, 2019.
- [2] 3GPP TR 38.855, "Study on NR positioning support," Rel. 16, 2019.
- [3] J. A. del Peral-Rosado, J. Saloranta, G. Destino, J. A. López-Salcedo, and G. Seco-Granados, "Methodology for simulating 5G and GNSS high-accuracy positioning," *Sensors*, vol. 18, no. 10, p. 3220, 2018.
- [4] R1-1900236, "Performance evaluation for hybrid positioning based on GNSS and NR," 3GPP, ESA, RAN1 AH-1901, Taipei, Taiwan, 2019.
- [5] ETSI TS 103 246-3, "Satellite Earth Stations and Systems (SES); GNSS based location systems; Part 3: Performance requirements," July 2015.
- [6] 3GPP TR 38.901, "Study on channel model for frequencies from 0.5 to 100 GHz," Rel. 14, Dec. 2017.
- [7] E. Domínguez, F. Simón, P. Thomas, Y. Zheng, E. Wittmann, D. Lekaim, M. Tossaint, and M. Jeannot, "ESAs multi-constellation regional system land users test-bed integrity algorithms experimentation results," in *Proc. ION GNSS*, Sep. 2013.
- [8] T. Creel, A. J. Dorsey, P. J. Mendicki, J. Little, R. G. Mach, and B. A. Renfro, "Summary of accuracy improvements from the GPS legacy accuracy improvement initiative (L-AII)," in *Proc. ION GNSS*, 2007.
- [9] E. Kaplan and C. Hegarty, *Understanding GPS: principles and applications*. Artech house, 2005.
- [10] Department of Defense (USA), "GPS standard positioning service performance standards," 2008.
- [11] V. Oehler, J. M. Krueger, T. Beck, M. Kirchner, H. L. Trautenberg, J. Hahn, and D. Blonski, "Galileo system performance status report," in *Proc. ION GNSS*, 2009.
- [12] European GNSS (Galileo), "Open service definition document," 2019.
- [13] S. Revnivykh, "GLONASS status and progress," in *Proc. ION GNSS*, Sep. 2008.
- [14] H. Lei, S.-H. Yang, Z.-G. Li, W.-H. Jiao, and Q.-W. Yang, "Orbit determination of COMPASS-M1 based on time synchronization among stations," in *Proc. ION GNSS*, Sep. 2009.
- [15] Septentrio, "Polarx3 specifications," Datasheet, 2008.
- [16] J. M. López-Almansa, J. Cosmen-Schortmann, P. Coutinho, and M. Toledo, "Parametric and statistical characterization of multipath errors for Galileo signals," in *Proc. ION GNSS*, Sep. 2007.
- [17] E. Domínguez, G. Seco-Granados, J. A. López-Salcedo, D. Egea, E. Aguado, D. Lowe, D. Naberezhnykh, F. Dervis, J. Boyero, and I. Fernandez, "Characterization of integrity threats in terrestrial applications using real signal captures," in *Proc. ION GNSS*, Sep. 2014.
- [18] J. A. del Peral-Rosado, G. Seco-Granados, S. Kim, and J. A. López-Salcedo, "Network design for accurate vehicle localization," *IEEE Trans. Veh. Technol.*, vol. 68, no. 5, pp. 4316–4327, May 2019.